Organization and Interaction of Cholesterol and Phosphatidylcholine in Model Bilayer Membranes

Paul A. Hyslop,*,‡ Benoit Morel,§ and Richard D. Sauerheber‖

Department of Central Nervous System Pharmacology, Lilly Research Laboratories, Indianapolis, Indiana 46285, Department of Engineering and Public Policy, Carnegie-Mellon University, Pittsburgh, Pennsylvania 15213, and Rees-Stealy Research Foundation, 2001 4th Avenue, San Diego, California 92101

ABSTRACT: The molecular organization of sterols in liposomes of 1-palmitoyl-2-oleoyl-*sn*-glycero-3-phosphocholine (POPC) at 37 °C is examined by utilizing the fluorescent analogue of cholesterol cholesta-5,7,9-trien-3β-ol (cholestatrienol). (1) Cholestatrienol is shown to be indistinguishable from native cholesterol in terms of its ability to condense POPC, as determined by (i) pressure/area studies of mixed-lipid monolayers and (ii) its ability to increase the order of POPC bilayers (determined by electron spin resonance studies) whether on its own or admixed with cholesterol at various ratios. (2) By analysis of the perturbation of the absorption spectra, cholestatrienol was found to be freely miscible in aggregates of cholesterol in buffer. In contrast, a lack of any detectable direct interaction of the sterol molecules in POPC bilayers was detected. (3) Fluorescence intensity and lifetime measurements of POPC/sterol (1:1 mol/mol) at various cholesterol/cholestatrienol molar ratios (0.5:1 up to 1:1 cholestatrienol/POPC) confirmed that sterol molecules in the membrane matrix were not associated to any great degree. (4) A quantitative estimate of how close sterol molecules approach each other in the membrane matrix was evaluated from the concentration dependence of the steady-state depolarization of fluorescence and was found to be 10.6 Å. From geometrical considerations, the sterol/phospholipid phase at 1:1 mol/mol is depicted as each sterol having four POPC molecules as nearest neighbors. We term this arrangement of the lipid matrix an "ordered bimolecular mesomorphic lattice". (5) The concentration dependence of depolarization of fluorescence of cholestatrienol in POPC liposomes in the absence of cholesterol yielded results that were consistent with the cholestatrienol molecules being homogeneously dispersed throughout the phospholipid phase at sterol/POPC ratios of less than 1:1. (6) From qualitative calculations of the van der Waals' hydrophobic interactions of the lipid species, the phospholipid condensing effect of cholesterol is postulated to arise from increased interpenetration of the flexible methylene segments of the acyl chains, as a direct result of their greater mutual attraction compared to their attraction for neighboring sterol molecules. (7) The interdependence of the ordered bimolecular mesomorphic lattice and the acyl chain condensation is discussed in an effort to understand the ability of cholesterol to modulate the physical and mechanical properties of biological membranes.

The major functions of cholesterol in the plasma membrane appear to involve minimizing the permeability to small molecules and ions (Demel et al., 1971) and modulating the physical and mechanical properties of the membrane (Stockton & Smith, 1976; Jacobs & Oldfield, 1979; El-Sayed et al., 1986). These effects of cholesterol arise from the reduction in the degrees of motional freedom of the acyl chains of the phospholipids (Stockton & Smith, 1976), resulting in an increased in-plane elastic stiffness and viscosity of the membrane (El-Sayed et al., 1986).

Cholesterol also can modulate the activity (Whetton et al., 1983; Connolly et al., 1986) and distribution of membrane proteins (Rottem et al., 1973). Also, heterogeneous phospholipid classes and species within the membrane matrix give rise to laterally inhomogeneous cholesterol distribution (de Kruyff et al., 1974) as well as to an asymmetric transbilayer distribution of cholesterol (Hale & Schroeder, 1982). These effects of cholesterol on plasma membrane structure and function appear to have wide pathological implications. For example, modulation of the cholesterol content of the plasma membrane influences platelet aggregation (McLeod et al., 1982). Also, manipulation of the fluidity and cholesterol

content of the lipid envelopes of both vesicular stomatitis (Pal et al., 1981) and HIV (Aloia et al., 1988; Crews et al., 1988) markedly influences the infectivity of these retroviruses.

Insights to the physical principles by which cholesterol modulates the molecular motion of the acyl chains have come from an understanding of both the organization and motional characteristics of the lipid components, utilizing model lipid membranes [Yeagle (1985) and references cited therein]. The cholesterol molecule is located with its hydroxyl in the ester carbonyl region of the hydrophilic/hydrophobic interface (Worcester & Franks, 1976) and its long axis perpendicular to the membrane surface. On the time scale of interest (i.e., with respect to acyl chain anisotropic segmental motion; Davis, 1983), the cholesterol molecule rotates unhindered about its long axis with a correlation time of about 100 ps (Taylor et al., 1981; Yeagle, 1981). The phospholipid molecules have much longer rotational correlational times ($\sim$10 ns), which preclude any long-lived complex with the sterol (Yeagle, 1981).

The rigid cholesterol molecule exhibits rapid, highly hindered angular fluctuations about its short axis with a rotational correlation time of around 500 ps (Taylor et al., 1982). The relatively rigid fused ring system and the nearly axially symmetric reorientation of cholesterol make it possible to describe its angular fluctuations in terms of a single molecular order parameter of 0.78 in DMPC liposomes at 37 °C (Dufourc et al., 1984). The segmental order parameter measurements of the acyl chain methylene deuterons from C_2 to C_{11} are about

---

0.45 and 0.7 in the absence and presence of cholesterol, respectively (Stockton & Smith, 1976; Dufourc et al., 1984).

Although the mechanism by which cholesterol decreases the acyl chain order remains elusive, it appears that the effect arises as a consequence of acyl chain/cholesterol interactions within the hydrophobic region of the membrane. This notion is supported by studies indicating that the phospholipid headgroup is apparently unnecessary for the condensation effect (Muller-Landau & Cadenhead, 1979) and that hydrogen bonding at the interfacial region is also not a prerequisite (Bittman et al., 1984).

There is some evidence that local molecular interactions between cholesterol and acyl chains contribute to the ordering effects of cholesterol, independent of the long-range organizational arrangement (Jain & White, 1977) of the components. For example, the ordering effects of cholesterol, as measured by ^{2}H NMR, are directly proportional to sterol incorporation from 5 to 35 mol % (Stockton & Smith, 1976), as are the effects of cholesterol on PC permeability (De Gier et al., 1968). However, pronounced nonlinear concentrational effects of cholesterol have been observed, for example, on lateral diffusion rates and vertical fluctuations of probes in PC bilayers (Yin et al., 1987) and on both the anisotropic bulk viscosity and the modulus of PC membranes (El-Sayed et al., 1986). Thus, both local and organizational contributions might influence the overall effects of cholesterol on phospholipid bilayers.

Information concerning the relative location of sterol molecules within the phospholipid phase has come from studies monitoring the behavior of fluorescent analogues of cholesterol (Rogers et al., 1979; Schroeder et al., 1981, 1987; Smutzer, 1988), calorimetry (Ladbrook et al., 1968; Mabrey et al., 1978), electron diffraction (Hui & Parsons, 1975), X-ray diffraction (Bourges et al., 1967; Lecuyer & Dervichian, 1969), and NMR (Darke et al., 1972). These studies all suggest that cholesterol may adopt particular arrangements with respect to the phospholipid molecules, such as a 1:1 stoichiometry (Presti et al., 1982a,b).

A complete understanding of the principles underlying the ability of cholesterol to modulate the physical properties of biological membranes will, of course, only come about when the appropriate equations of state are generated for all the polydispersed components in the membrane. Even for simple binary mixtures of cholesterol and phospholipids, it will be necessary to understand the organization of the components within the lipid matrix, the relative strengths of the interactions between the molecular segments, the degree of cooperativity of the interactions, and finally the interdependence of these effects.

In this study, we utilize a fluorescent analogue of cholesterol to address some of these issues. Using depolarization of fluorescence to measure the rate of excitation energy migration between chromophores, we determine the average separation distance between sterol molecules, in order to evaluate the distribution of sterol molecules within the lipid matrix. The data are utilized to construct a molecular model of the hydrophobic region of the membrane on the fluorescence time scale at 1:1 sterol to phospholipid and in conjunction with experimental data obtained at lower sterol/phospholipid ratios, cooperative interactions among sterol molecules are investigated. Finally, we combine these and other experimental observations to advance a chemical thermodynamic hypothesis of cholesterol–phospholipid interaction.

MATERIALS AND METHODS

(*1*) *Preparation of Cholestatrienol.*[1] Cholestatrienol was prepared by mercuric acetate oxidation of 7-dehydrocholesterol (Sigma, St. Louis, MO), as described by Antoucci et al. (1951). The product was recrystallized from diethyl ether/ethanol and HPLC performed on C18RP Zorbax using methanol/acetonitrile (1:1), 2 mL/min, as the mobile phase. The retention times of cholestatrienol and 7-dehydrocholesterol [identified by UV absorption spectra given in Schroeder et al. (1984)] were 11.1 and 18.0 min, respectively. The molar absorbance of cholestatrienol eluting from the column was 11 700 cm^{-1} at 323 nm, in accordance with published values (Rogers et al., 1979; Schroeder, 1984). The sterol was stored at 1.5 mM at –20 °C under argon in the eluting solvent. No significant deterioration of the material occurred for at least 2 years.

(*2*) *Preparation of Lipids.* POPC (Avanti Polar Lipids Inc., Birmingham, AL) was used without further purification, since no detectable UV absorbance was detected at >300 nm of a 10 mM stock solution in ethanol. Cholesterol (Eastman Kodak Co., Rochester, NY) was purified by HPLC and stored as described for cholestatrienol (retention time = 20.5 min) at 1.5 mM. All lipids were filtered through nylon 0.22-μm filters prior to use.

(*3*) *Preparation of Liposomes.* Organic solvent was completely removed from aliquots of the lipid mixtures in glass tubes under a stream of nitrogen; 1 mL of filtered buffer (150 mM NaCl, 1 mM EDTA, 10 mM MOPS, pH 7.4, at 37 °C) was then added. The tubes were then flushed with nitrogen for 10 min, sealed, and mechanically shaken (five oscillations/s) for 72 h. At the end of this period, the tubes were sonicated in a Rai Research ultrasonic bath (Fisher Scientific) for 30 s and shaken for a further 24 h. This procedure resulted in no loss of cholestatrienol, complete dispersion of the lipids, and reasonably consistent experimental data between batches of lipid dispersions.

(*4*) *Preparatioin of Sterol Aggregates in Buffer.* Various mixtures of cholesterol and cholestatrienol (10 mM in methanol) were injected into rapidly stirring buffer (50 μM final concentration) and sonicated for 5 min, under nitrogen. Cholestatrienol fluorescence anisotropy, intensity, and fluorescence lifetime were measured over the range 1:200 up to 1:10 (mol of cholestatrienol/mol of cholesterol).

Cholesterol aggregates in buffer apparently form microcrystals of pure cholesterol and cholesterol monohydrate (Renshaw et al., 1983). In this study, it is established that cholestatrienol mixes readily with these phases of cholesterol. At low (1:200) cholestatrienol/cholesterol ratios, which would not be expected to melt the putative cholesterol crystals, significant cholestatrienol molecular motion is observed from studies of the depolarization of the cholestatrienol emission (see section 9 under Results). With respect to the cholestatrienol molecules at least, the phase therefore appears to be more mesomorphic than crystalline. A reasonably high degree of molecular collinearity and symmetric orientation typical of cholesteric mesophases would therefore be expected. As an approximation, the relative cholestatrienol concentration in these cholesterol aggregates is therefore scaled in terms of the cross-sectional areas of these molecules, enabling a direct comparison with studies with a two-dimensional lipid matrix of cholestatrienol in POPC.

R_0 was determined for cholestatrienol in cholesterol aggregates at each concentration, from the same parameters as

---

[1] Abbreviations: cholestatrienol, cholesta-5,7,9-trien-3β-ol; POPC, 1-palmitoyl-2-oleoyl-*sn*-glycero-3-phosphocholine; pyrenyl-PC, 1-palmitoyl-2-(10-pyren-1-yl-10-ketodecanoyl)-*sn*-glycero-3-phosphocholine; MOPS, 3-(*N*-morpholino)propanesulfonic acid.

for POPC, adjusted only for quantum yield differences (calculated from the measured fluorescence lifetimes) at each data point.

(5) *Absorbance Measurements.* Absorbance measurements were performed on a Perkin-Elmer Lambda 4C spectrophotometer, with a modified photomultiplier tube in close proximity to the sample cuvette to assist collection of light from scattering samples. The shape of the absorption spectrum of cholestatrienol in POPC liposomes (1:1 mol/mol) was monitored to assess the degree of electronic interaction of the π orbitals between chromophores. Scattering of the incident light gives rise to errors in both the absolute and the wavelength dependence of the absorbance. The magnitude of these artifacts can be assessed by comparison to absorbance data obtained with pyrenyl-PC (Molecular Probes Inc., Eugene, OR) which randomly distributes in POPC bilayers (Hresko et al., 1986). At relatively low concentrations (<10 mol %) of pyrenyl-PC in POPC, the probability of electronic interactions between the pyrenyl molecular orbitals is likely to be minimal. (No differences in the absorption spectra were observed at 5 or 10 mol % pyrenyl-POPC.) The apparent hypochromicity of 7.5 mol % pyrenyl-PC spectra in POPC liposomes was determined as a ratio of the absorbance of an identical aliquot of the liposome suspension dissolved in ethanol to that of the portion of the UV spectrum pertinent to cholestatrienol. The corrected cholestatrienol absorbance spectra in POPC (1:1 mol/mol) were then obtained from the data. The absorbance spectra of 5–50 μM cholestatrienol in cholesterol aggregates were taken and averaged over five separate samples, following subtraction of the absorbance of identical solutions containing aggregates with cholesterol stoichiometrically replacing cholestatrienol.

(6) *Molecular Area Determinations.* Surface pressure measurements were performed by utilizing a Kruss K8451 surface balance. Monolayers of a lipid film were dispersed into 10 mL of buffer contained in a 5 cm diameter glass dish, maintained on a 37 °C hotplate. The instrument was calibrated with water and methanol as surface tension standards. Lipid mixtures in acetonitrile/methanol were added to the dish in varying aliquots, such that the small amounts of solvent did not significantly alter the buffer surface pressure. Following breaking the surface with the balance ring and noting the apparent surface tension, the dish was rinsed in 70% ethanol followed by water before adding fresh buffer for the next determination. Pressure/area curves were constructed, and the molecular areas were interpolated at 20 mN·M^{-1}, representing the approximate equilibrium lateral pressure in liposomes (Marcelja, 1974).

(7) *Electron Spin Resonance (ESR) Spectroscopy.* Liposome suspensions (4 mM) were labeled with 5 nmol of 5-nitroxide stearate spin-label [I(12,3); Syva Co., Palo Alto, CA] diluted into 70 μL of lipid sample. ESR spectra were recorded at 37 °C with a Varian E-104A Century Series ESR spectrometer. The order parameters S, $S(T_{\parallel})$, and $S(T_{\perp})$ are sensitive to the flexibility of membrane-incorporated spin-labels undergoing rapid anisotropic rotational motion about a unique symmetry axis (Gordon & Sauerheber, 1977). Each may be measured from the outer and inner hyperfine splittings observed in the ESR spectra of the I(12,3)-labeled membranes as described previously (Sauerheber et al., 1977). The isotropic hyperfine coupling constants $a_{N'}$ and a_N are obtained from the ESR spectra of the probe in the membrane and crystal states, respectively, and are sensitive to the polarity of the environment of the probe (Hubbell & McConnell, 1969).

(8) *Fluorescence Lifetime Measurements.* (*A*) *Time Domain.* Picosecond pulses (1–2 ps FWHM) were generated by synchronously pumping a Rhodamine 6G dye laser with the second harmonic of a CW mode-locked Nd^{3+} YAG laser (Quantronix 116, mode locked at 38 MHz). The dye laser pulses are amplified by a three-stage longitudinally pumped pulsed dye amplifier with a Quanta Ray DCR-2 Nd^{3+} YAG laser (100-mJ pulses at 532 nm). The output (1 mJ/pulse) is frequency doubled to 300 nm and used to excite the cholestatrienol sample. The remaining red light is delayed and used as a timing marker. Fluorescence emission is detected at 90° to the incident pulse with a Hammatsu C979 streak camera, whose output is recorded by an EGG Intensified Reticon, interfaced with an LS1-11/23 computer. The position and intensity of the red prepulse are also analyzed, and acceptable data are shifted and added to memory at the laser repetition rate of 20 Hz. Time calibration and nonlinearity calibrations for this system have been described (Su & Simon, 1987). On average, 500 decays of 2-ns durations were averaged for each sample. All decay kinetics were determined by convolving the desired functional form with the prepulse recorded by the streak camera (Su & Simon, 1987). Decays were fitted to the appropriate sum of weighted exponential terms that resulted in minimal residual deviation between the data and the fit.

(*B*) *Frequency Domain.* Phase shift and demodulation of cholestatrienol emission were measured with an SLM 48000 multifrequency cross-correlation spectrophotofluorometer (SLM Aminco, Urbana, IL). The sample was excited at 325 nm with vertically polarized light by use of a 2-mW He/Cd laser (Omnichrome, Chino, CA), a Pockels cell light modulator, and a Q-switched polarizer, over the frequency range 10–150 MHz, in steps of 10 MHz. 2,5-Diphenyloxazole was used as a lifetime reference (1.4 ns in ethanol; Lakowicz et al., 1981), chosen for its similarity of emission spectrum to that of cholestatrienol. Emission was observed through Corning 375 filters and a glan prism polarizer at 54.7°.

The contribution and lifetimes of the emitting species in the sample were calculated with the software supplied with the instrument. Briefly, phase and modulation lifetimes were calculated from the real and imaginary components of the Fourier transform integral of the impulse response and harmonic excitation. The impulse response of emission of a multiple-lifetime population of chromophores is the weighted sum of exponential decay terms where the fractional intensities are the products of the preexponential weighting factors and lifetimes (Gratton, 1984). Experimental multifrequency data were compared to calculated values obtained for the desired model where floating parameters of lifetime and fractional intensity were iteratively varied in a direction that minimized the reduced χ^2.

(9) *Steady-State Fluorescence Intensity Measurements.* Fluorescence spectroscopy was performed on either a Model 4800 or a Model 48000 spectrofluorometer (SLM Aminco, Urbana, IL). Excitation intensities were delivered through the grating monochrometer at 323 nm, 0.5-nm band-pass. The sample (1.5 mL) was contained in a stirred, thermostated (37 °C) quartz 1-cm cuvette. Emission intensities were observed through the monochrometer with the emission polarizers rotated to 55.7°. Spectral data were stored on the IBM PS-60. Emission wavenumber intensity correction and integration were performed with the software supplied with the instrument.

Fluorescence intensity measurements in the standard 90° format of cholestatrienol in PC are difficult to directly quantitate due to the complex effects of scattering of both the

excitation and emission light by the liposomes. The following approach was therefore adopted: At all cholestatrienol/total lipid ratios, both the concentration of cholestatrienol (2.5 μM) and that of the total lipid (100 μM) in the sample cuvette were kept constant. This manipulation involves admixing liposome suspensions with cholesterol substituted for cholestatrienol and assumes minimal exchange of sterol between the admixed liposomes. During the time course of temperature equilibration and measurement following mixing (usually 4–5 min), sterol is not expected to exchange to a significant degree ($t_{0.5}$ = 90 min; Backer & Dawidowicz, 1979). We verified this observation in our system by attempting to observe a reduction in the rate of energy transfer between cholestatrienol molecules upon addition of a large excess of cholesterol/POPC liposomes (1:1) to the sample. No significant increase in the degree of fluorescence polarization was observed in samples containing 1:1 POPC/cholestatrienol diluted 50-fold with nonfluorescent liposomes for at least 8 min.

(10) Fluorescence Depolarization Measurements. Two channel depolarization measurements corrected for instrumental artifacts were performed, and the resulting steady-state fluorescence depolarization and anisotropies were calculated as described by Lakowicz (1983). Emission was detected through Corning 375 filters. All emission intensities were corrected for background fluorescence/stray light (typically <5% of signal intensities) by subtraction of similar intensities obtained from identical liposome solutions containing cholesterol stoichiometrically replacing cholestatrienol.

The limiting anisotropy, r_0, was obtained (0.37) from measurement of the corrected steady-state anisotropy of cholestatrienol (1 × 10^{-6} M) in propane-1,3-diol at –40 °C and was in good agreement with values obtained for dehydroergosterol (Schroeder et al., 1987). Analysis of the excitation polarization spectrum yielded a decrease in the value of r_0 only at wavelengths below 310 nm, indicating relatively collinear absorption and emission oscillators for the two long-wavelength absorption bands.

(11) Time-Dependent Decay of Fluorescence Anisotropy Measured by Multifrequency Differential Polarized Fluorometry. Multifrequency phase and modulation measurements were performed with dual-channel emission detectors and vertically polarized modulated light from the He/Cd laser. The emission polarizer of one channel was rotated to give phase angle and modulated amplitude ratios of the vertically and horizontally polarized intensities with reference to the horizontal polarizer orientation of the second channel. The phase and modulation frequency file was compiled between 10 and 160 MHz at 5-MHz steps, while the depth of excitation modulation varied from 1.7 at 10 MHz to 0.4 at 160 MHz.

The fluorescence anisotropy for an asymmetric body is expected to decay as a sum of exponentials:

$$r(t) = r_0 \sum g_i e^{-t/\phi_i} \tag{1}$$

where g is the fractional anisotropy loss for a particular rotational correlation time (ϕ). In the case of cholesterol in lipid bilayers, isotropic rotation about the long axis and anisotropic rotations around the short axis appear to adequately describe the molecular motion (introduction). The correlation times of these two processes are within a factor of 5 (introduction), and their relative contributions to the time-dependent fluorescence anisotropy decay would be difficult to resolve. However, the fluctuations about the short axis beyond a relatively small cone angle around the membrane normal are energetically so unfavorable (Dufourc et al., 1984) that residual fluorescence anisotropy (r_∞) should result from the anisotropic rotations about the short axis and should be readily
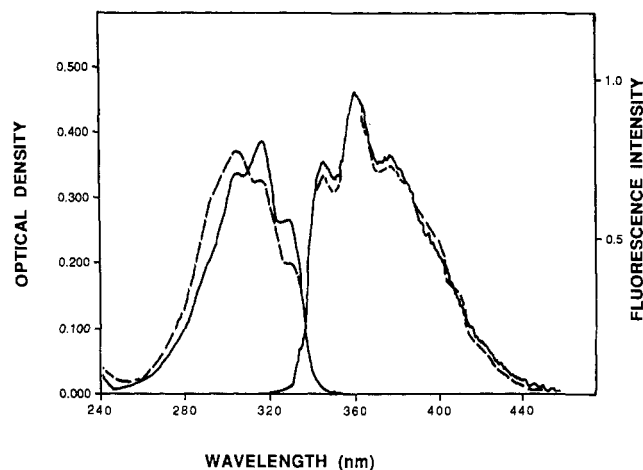

FIGURE 1: (—) Absorption and corrected emission spectra of 5 × 10^{-5} M cholestatrienol in ethanol. Emission wavenumber conversion was performed for 2-nm band-pass. (- -) Absorption and corrected emission spectra (normalized) of 5 × 10^{-5} M cholestatrienol aggregates in buffer.

obtained to a reasonable degree of precision from phase and modulation data.

Analysis of r_∞ utilizing an apparent single rotational correlation time can be obtained from the time-dependent anisotropy decay:

$$r(t) = (r_0 - r_\infty)e^{-t/\phi} + r_\infty \tag{2}$$

$r(t)$ was obtained from the experimental multifrequency data following transformation of the impulse responses of the vertically and horizontally polarized intensities into the frequency domain.

The fixed parameters for this analysis were the lifetime and the limiting anisotropy, corrected for instrumental and sample artifacts, while best-fit solutions from the dynamic data for cholestatrienol at 5 mol % in POPC/sterol liposomes were obtained for floating values of the rotational correlational time and r_∞.

It is of interest to note that if the transition dipoles of cholestatrienol are oriented either perpendicular or parallel to the long molecular axis, the isotropic or anisotropic rotations, respectively, will be relatively inactive in depolarizing the emission. The data obtained by time-resolved anisotropy decay will therefore contain information about the relative orientations of the dipoles with respect to the molecular axes.

The average amplitude ($\langle\theta\rangle_{max}$) of the angular distribution of a chromophore around an axis of hindered rotation at times that are long compared with the fluorescence lifetime can be estimated according to Weber (1978):

$$\cos^2 \langle\theta\rangle_{max} = [1 + 2(r_\infty/r_s)]/3 \tag{3}$$

The corresponding order parameter (S) of the molecular segment containing the emission dipole is given by

$$S = (3 \cos^2 \langle\theta\rangle_{max} - 1)/2 \tag{4}$$

THEORETICAL AND EXPERIMENTAL CONSIDERATIONS

(1) Calculation of the Forster Critical Distance, R_0. Molecules such as cholestatrienol that possess significant overlap of absorption and emission frequencies (Figure 1) may participate in intramolecular dipole–dipole (singlet) resonance transfer of the emission radiation. The rate of transfer of the emission radiation between cholestatrienol molecules is inversely proportional to the sixth power of their separation distance R and also to the magnitude of the spectral overlap integral $J\nu$ (Forster, 1948).

The constant terms in Forster's equation are combined, and the Forster critical distance is defined where the probabilities of emission and energy transfer are equal (R_0):

$$R_0^6 \ (\text{Å}) = (9.79 \times 10^3)((\langle K^2 \rangle n^{-4} \Phi J\nu)^{1/6} \quad (5)$$

where Φ is the quantum yield, n is the mean refractive index over the region of spectral overlap, $\langle K \rangle$ is the average orientation of the electric vectors of the absorption and emission dipole, and $J\nu$ is given by

$$J\nu = \int F \, d(\nu) \, a(\nu) \, d\nu \, \nu^4 \, d\nu \quad (6)$$

$F \, d(\nu)$ is the sum of the corrected normalized fluorescence intensity over each wavenumber interval; $a(\nu)$ is the sum of the molar absorbancies at each wavenumber interval over the absorption band. The spectral overlap integral for cholestatrienol ($J\nu$) was calculated from eq 6 and was found to be $2.964 \times 10^{-16} \ \text{M}^{-1} \ \text{cm}^3$.

The fluorescence quantum yield ($\Phi = \tau/\tau_0$) of cholestatrienol in POPC was estimated indirectly from the measured fluorescence lifetime (τ) and the calculated radiative lifetime in the absence of competing deactivation processes (τ_0). τ_0 was obtained by measurement of the fluorescence lifetime in ethanol, while Φ was determined in this solvent by comparison to that of quinine sulfate in the usual manner (Lakowicz, 1983), yielding $\tau_0 = 5.58 \times 10^{-9}$ s.

In addition, τ_0 was estimated according to Strickler and Berg (1962) from the spectral characteristics of the molecule, modified for the optical dispersion of the medium (Birks & Dyson, 1963). Since the absorption and emission spectra have reasonable symmetry and the absorption transition is moderately strong, τ_0 should be obtained to ±10% (Birks & Dyson, 1963). Estimations of the appropriate indices of refraction (n) for the hydrocarbon interior of the bilayer at 37 °C were obtained from the estimate of n for mineral oil at 20 °C, measured at the d line of sodium (Larsen & Berman, 1934), and corrected for wavelength dispersion and temperature. The spectral and refractive index values yield $\tau_0 = 5.63 \times 10^{-9}$ s, in good agreement with that obtained from intensity and lifetime measurements. The fluorescence quantum yield of cholestatrienol in POPC liposomes at 37 °C, calculated from the radiative and fluorescence lifetimes, is therefore 0.111.

The electric vector (and hence the induced transition dipole) of the exciting quanta lies along the C=C bond axis of ethylene for efficient absorption (Bowen, 1954). The conjugated triene π orbitals all lie within a plane bounded by carbon atoms 4–14 of the A, B, and C rings of the sterol, and the direction of the absorption dipole moment must therefore also be constrained to this plane. This is also approximately correct for the emission dipole, which is displaced 13° from the absorption dipole, calculated as described by Lakowicz (1983) from r_0 (see section 11 under Materials and Methods).

It remains only to determine the angle the transition dipoles subtend within this plane, relative to the molecular axes of cholestatrienol. Dynamic depolarization measurements of cholestatrienol (see section 8 under Results) indicate that the molecular motions contributing to the decay of fluorescence anisotropy are highly hindered, and therefore, the direction of the transition dipoles must be more aligned in the direction of the long rather than the short molecular axis. The wobble ($\langle \theta \rangle_{max}$, eq 3) and axial rotation of the molecule displace the transition moments within a cone of half-angle of 23.1°, and the appropriate geometrical arrangement of these dipoles (Figure 2) within the membrane matrix corresponds to model 6.(iv) given in Dale and Eisinger (1975).

$\langle K \rangle$ is obtained by numerical integration over all possible relative orientations of the dipoles within the constraints in-

dicated in Figure 2. Because the distribution of chromophores is two-dimensional rather than three-dimensional, the average value of the orientation parameter is $\langle K^{2/3} \rangle^3 = 0.87$. Substituting this calculated value for K^2 into eq 5, we arrive at $R_0 = 13.2$ Å.

(2) *Use of Energy Transfer To Probe Inter-Sterol Distances in the Bilayer.* The efficiency (E) of energy transfer between two chromophores separated by a distance, R, is given by

$$E = R_0^6/(R_0^6 + R^6) \quad (7)$$

It is immediately apparent from eq 7 that, for cholestatrienol located in membranes, energy transfer across the bilayer halves is very inefficient (<2%), since the minimum distance separating the centers of gravity of the π orbitals between two molecules located in opposite monolayers is >25 Å. Energy transfer to neighboring chromophores, on the other hand, whose centers are separated, for example, by the diameter of a phospholipid molecule, results in suitably efficient transfer of the excitation (26%) and increases to ~98% as the chromophores approach each other close to their limiting separation distance of approximately two molecular radii, or about 7 Å.

The diffusion coefficient of phospholipid and cholesterol molecules in liposomes with 50 mol % cholesterol at 37 °C is approximately $1.5 \times 10^{-8} \ \text{cm}^2/\text{s}$ (Golan et al., 1984), which agrees well with the predicted Stokes–Einstein value from the membrane viscosity measurements of El-Sayed et al. (1987). Thus, a lipid molecule diffuses for 333 ns during a jump length of one phospholipid diameter (Einstein–Smoluchowski equation). It is clear from these considerations that molecular organization probed during the cholestatrienol fluorescence time scale will not be particularly sensitive to diffusional averaging and that rates of energy transfer will be strongly influenced by separation distances of sterol molecules within each monolayer.

(3) *Concentration Dependence of Depolarization of Fluorescence by Energy Transport between Cholestatrienol Molecules in PC/Sterol Liposomes.* Energy transfer between cholestatrienol molecules results in hopping of the excitation between chromophores (energy transport). Each nonradiative transfer step between molecules of different relative orientations alters the helicity of the emitted photon. The dependence of the polarization of fluorescence and chromophore concentration for vertically polarized excitation can be expressed according to Weber (1954):

$$1/p - 1/3 = (1/p_0 - 1/3)[1 + (3/2)\langle \sin^2 \theta_T \rangle \langle n \rangle] \quad (8)$$

where $\langle n \rangle$ is the average number of intramolecular transfers of the excitation energy from the original excited chromophore into the ensemble before emission. For a two-dimensional array of cholestatrienol molecules in a monolayer that are not necessarily randomly distributed

$$\langle n \rangle = \int_L^\infty dR \ (R_0/R)^6 2Rm \int d_T K^2 \quad (9)$$

where m is the number of molecules per unit area, d_T is the transfer depolarization factor for a given orientation of chromophore donor and acceptor pairs, and L is the average minimum attainable distance separating chromophores, or "distance of closest approach". Therefore

$$\langle n \rangle = (1/2)mR_0^2(R_0/L)^4(\langle K^2 \rangle \langle d_T \rangle) \quad (10)$$

$$\langle \sin^2 \theta_T \rangle = \langle K^2 \rangle^{-1} \int d_T \sin^2 \theta_T K^2(\theta_T) \quad (11)$$

The average value of $\sin^2 \theta_T$ is calculated numerically, as described for model 6.(iv) by Dale and Eisinger (1975), for chromophores with the constraints of the geometric configu-
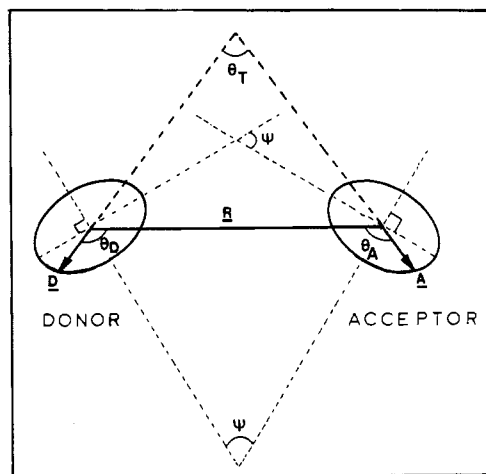
FIGURE 2: Geometry of donor/acceptor transition moment vector pairs (D and A) and the direction joining them (R) of cholestatrienol molecules in POPC liposomes. ψ is the angle between the planes in which these vectors are constrained. The approximate orientation of the transition dipoles relative to the molecular axis and the membrane normal is described in the text. The Monte-Carlo numerical integrations for calculation of $\langle K^2 \rangle$ and $\langle \sin^2 \theta_T \rangle$ are performed with the geometrical constraints $0 < \psi < 46.2°$ and $0 < \theta < 2\pi$.

ration given in Figure 2. This yields $\langle \sin^2 \theta_T \rangle = 0.6$, and therefore

$$1/p - 1/3 = (1/p_0 - 1/3)[1 + 0.41(R_0/L)^4 mR_0^2] \quad (12)$$

Thus, a plot of $1/p$ as a function of chromophore density scaled to R_0^2 yields both p_0 and the ensemble average separation distance of the cholestatrienol molecules in the POPC/sterol lattice.

(4) Quenching of Fluorescence Due to Energy Traps Created by Hybrid Chromophores. When chromophores are close enough such that their electronic wave functions overlap, the hybrid nonfluorescent chromophores create an energy trap for migrating photons from the uncomplexed fluorescent species. For this situation, numerical solutions have been obtained (corrected for excluded volume interactions) for the quenching of donor chromophores by acceptor hybrids in a two-dimensional continuum (Snyder & Freire, 1982) of the form

$$\tau_q/\tau = \exp[B(\langle R_0 \rangle/L)C] \quad (13)$$

where τ_q is the radiative fluorescence lifetime measured in the presence of quenchers. The decay constant term was generated from a third-order polynomial expression:

$$B(\langle R_0 \rangle/L) = \sum_{i=0}^{3} a_i (R_0/L)^{-i} \quad (14)$$

where

$$a_0 = -3.448 \quad a_1 = -0.4021$$
$$a_2 = 4.136 \quad a_3 = -1.668$$

The correct scaling of the decrease in relative fluorescence lifetime (obtained as a function of the relative chromophore concentration) to the estimated density of energy traps formed in the membrane matrix is obtained by iterative curve fitting of the experimental data to eq 13, utilizing appropriate values of R_0/L.

(5) Fluorescence Depolarization Studies of Cholestatrienol in POPC Liposomes in the Absence of Cholesterol. It is of interest to determine whether sterols disperse evenly throughout the phospholipid phase at sterol/POPC ratios of <1:1 or whether sterol clustering occurs forming sterol-rich and -poor domains, respectively. Furthermore, we should like to specifically explore the possibility that cooperative effects

of sterol/phospholipid clusters might contribute to the ordering/condensing effects of cholesterol.

Our major energy-transfer study utilizing depolarization of fluorescence (see section 3 under Theoretical and Experimental Considerations) is conducted at an equimolar sterol/phospholipid ratio for two reasons: First, geometrical considerations greatly assist in the interpretation of experimental data. For example, at lower sterol concentrations (where a large number of arrangements could yield the same ensemble average distance of closest approach), this type of analysis for organization of membrane components would be obviously more ambiguous. Second, the sterol concentration of liposomes not only has a marked effect on the ordering of phospholipid molecules but also influences the motions of the sterol molecules themselves (Taylor et al., 1982). By varying the cholestatrienol concentration under conditions where the sterol content of the liposomes is constant, any changes in energy-transfer efficiency due to varying the molecular orientation, rotational rate, and lifetime will be minimized by this approach. In this manner, information concerning the distance of closest approach and the behavior of the various photophysical phenomena as a function of replacing cholesterol sites in the lipid lattice with cholestatrienol molecules is obtained.

If, however, the concentrational dependence of fluorescence depolarization is also conducted with cholestatrienol over the same molar ratio to POPC as before but without addition of cholesterol to maintain the total sterol/POPC at 1:1, then, by comparison to the above data set, the relative distribution of cholestatrienol molecules throughout the bulk lipid phase (as a function of increasing mole fraction sterol) can be obtained.

The calculated values of $\langle K^2 \rangle$, R_0, and $\langle \sin^2 \theta_T \rangle$ for cholestatrienol at any given sterol:phospholipid ratio is determined by reevaluation of $\langle \theta_{max} \rangle$ calculated directly from the molecular order parameter data obtained by Taylor et al. (1982) and the measured fluorescence lifetime. From these values, and the determined R_0/L, the corrected depolarization value at each chromophore concentration is evaluated. The correct scaling of the chromophore concentration for any given sterol/phospholipid ratio is estimated from the appropriate molecular areas for condensed and uncondensed POPC (see section 2 under Results) and mole fractions of each component present.

(6) Liquid-Lattice Polymer Solution Theory and Cholesterol–Phospholipid Interaction. The application of polymer solution theory (Flory, 1952) to dispersions of cholesterol in phospholipid bilayers may be applied by utilizing the following criteria: Each acyl chain could be considered to be arms of a macromolecular complex, created by the lyotropic liquid crystalline continuum of phospholipid molecules. Acyl chains consist of flexible segments, which experience close proximity to other acyl chains on the same or neighboring phospholipid molecules, in an analogous manner to the flexible interpenetrating segments of a concentrated solution of polymeric macromolecules. The cholesterol molecule, on the other hand, can be viewed as a stack of hard, noninterpenetrating rigid spheres, analogous to molecules of solvent in which polymers under study are suspended. The use of a lattice approach in the development of Flory's theory seems particularly appropriate in this case.

If a cholesterol molecule behaves as a "good solvent", then acyl chain segments will experience an increase in their excluded volume and a corresponding decrease in the intramolecular expansion factor (Flory & Krigbaum, 1950; Tanford, 1961). If, on the other hand, cholesterol behaves as a "poor solvent" for acyl chains, the reverse will be true, since there

Table I: Isotropic Hyperfine Coupling Constants for I(12,3)-Labeled POPC Liposomes at 37 °C with or without Sterols (1:1) at Various Cholesterol/Cholestatrienol Ratios

system	$a_{N'}$
PC	14.90
PC:cholesterol:cholestatrienol (1:0.25:0.75)	15.40
PC:cholesterol:cholestatrienol (1:0.50:0.50)	15.33
PC:cholesterol:cholestatrienol (1:0.75:0.25)	15.39
PC:cholesterol (1:1)	15.33
PC:cholestatrienol (1:1)	15.4

will be a preference for segment–segment contact between segments on the same or neighboring phospholipid molecules. The relative strengths of these molecular interactions, as they relate to the relevant thermodynamic parameters (heat and entropy functions), can be described in terms of the Flory interaction parameter X (Flory, 1952) between both like (X_{11}, X_{22}) and unlike (X_{12}) species in the interacting mixtures.

Attempts to evaluate X_{12} for whole segments of interacting polymeric macromolecules have been described for polymer blends in order to predict polymer compatibility (Krause, 1978). The interaction parameter between molecules of comparable size (such as cholesterol and acyl chains) could be written in terms of Hildebrand solubility parameters (Hildebrand & Scott, 1962, Krause, 1978):

$$X_{12} = (V_r/RT)(\partial_1 - \partial_2)^2 \tag{15}$$

where ∂_1 and ∂_2 are the Hildebrand solubility parameters of two interacting species of molar volumes V_r, respectively.

Furthermore, the solubility parameters predicting polymer–polymer compatibility could be calculated from the sum of the molar attraction constants over all segments of the molecule ($\sum F_i$), their density (p), and molecular weight (M), as indicated by Krause (1978):

$$\partial = p\sum F_i/M \tag{16}$$

The value of the molar attraction constants of each carbon segment of cholesterol and acyl chain can be directly obtained from data first described by Small (1953) and later modified by Hoy (1970). It should therefore be possible from these relationships to qualitatively determine the effect of a juxtaposed cholesterol molecule on the degree (positive or negative) of interpenetration of neighboring acyl chain segments of the phospholipid molecules.

Results

(1) ESR Studies of Cholestatrienol/Cholesterol-Containing Liposomes. Order parameters ($S_{T_\parallel}$ and $S_{T_\perp}$) obtained from the ESR spectra of liposomes labeled with I(12,3) were plotted as a function of increasing molar ratio of either cholesterol or cholestatrienol (Figure 3, panel A). No apparent difference in the ability of the two sterols to influence any of the order parameters between 10 and 50 mol % sterol was observed.

ESR order parameters of POPC liposomes containing 50 mol % total sterol were plotted as a function of the mole fraction of cholestatrienol to total sterol (cholestatrienol plus cholesterol). Here (Figure 3, panel B), the ability of the two sterols to influence the order parameters was additive. The calculated isotropic hyperfine coupling constants $a_{N'}$ (Table I) were measured from the ESR spectra of I(12,3)-labeled liposomes of various composition. Again, the ability of the two sterols to influence $a_{N'}$ were both similar and additive.

These data contribute further to the body of literature confirming that cholestatrienol influences the motional and organizational properties of phospholipid liposomes in a manner similar to that of cholesterol (Rogers et al., 1979; Schroeder, 1984). Furthermore, it was necessary for this work

MOLAR RATIO STEROL/PHOSPHOLIPID
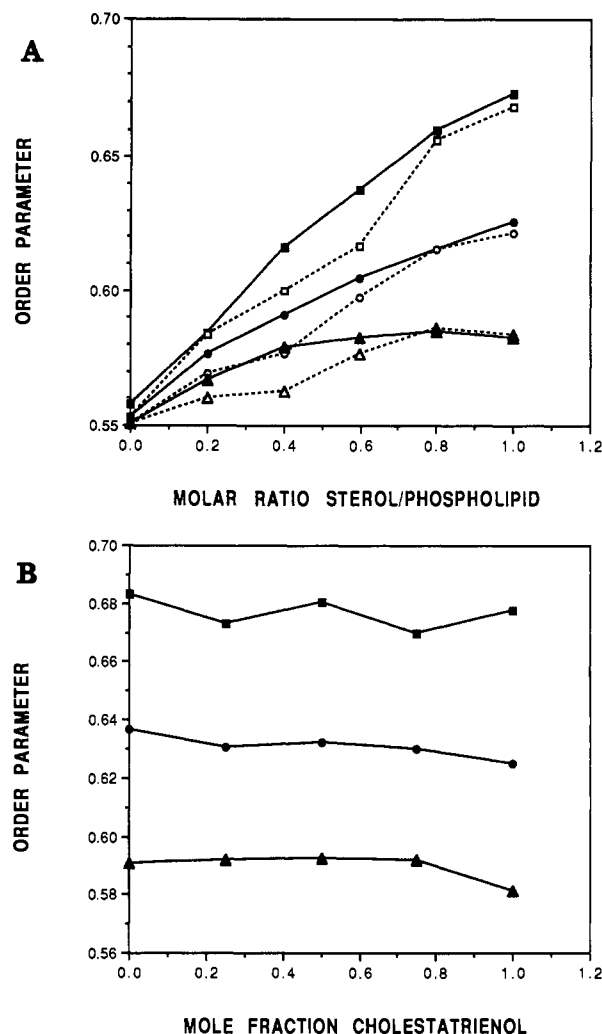

MOLE FRACTION CHOLESTATRIENOL

FIGURE 3: (Panel A) ESR order parameters for I(12,3) nitroxide stearate labeled POPC liposomes containing various cholesterol (—) or cholestatrienol (‐‐) concentrations. $S(T_\parallel)$ (■) and $S(T_\perp)$ (▲) are the order parameters obtained from the outer and inner hyperfine splittings, respectively. S (●) is the polarity-corrected order parameter obtained from the outer splitting and the respective isotropic hyperfine coupling constants. (Panel B) ESR order parameters [$S(T_\parallel)$ (■), $S(T_\perp)$ (▲), and S (●)] of I(12,3)-labeled POPC liposomes at 1:1 sterol/POPC, containing various cholesterol/cholestatrienol ratios.

to determine that the ordering effects of mixtures of the two sterols on POPC liposomes were additive.

(2) Pressure/Area Measurements. Surface pressure measurements are plotted as a function of added lipid (Figure 4). The pressure/area curves for cholestatrienol and cholesterol alone or admixed with POPC (1:1) were identical, within experimental error. The pressure/area curve for pure POPC is also shown. The mean molecular areas of the lipid components within the liposomes used in these studies were calculated at a surface pressure of 20 mN·m⁻¹.

Sterols and POPC demonstrated mean molecular areas of 39 and 66 Å²/molecule, respectively, and both sterols effectively condensed POPC in 1:1 lipid mixtures to 59 Å²/molecule. These data were utilized to calculate theoretical molecular densities in the liposome lattice.

(3) Absorption Spectra of Cholestatrienol/Cholesterol Aggregates in Buffer. The absorption spectra of associated and monomeric cholestatrienol molecules in buffer and ethanol, respectively, demonstrated that electronic overlap of the π orbitals resulted in distinct absorbance spectra (Figure 1, dashed line). The apparent absorbance of the associated hybrid cholestatrienol molecules over the region of the ab-
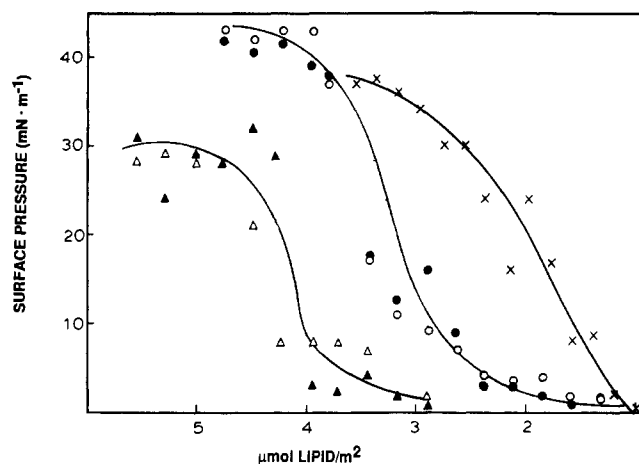
FIGURE 4: Surface pressure measurements at 37 °C performed on various lipid monolayers: (×) POPC; (●) POPC/cholesterol, 1:1; (○) POPC/cholestatrienol, 1:1; (▲) cholesterol; (△) cholestatrienol.
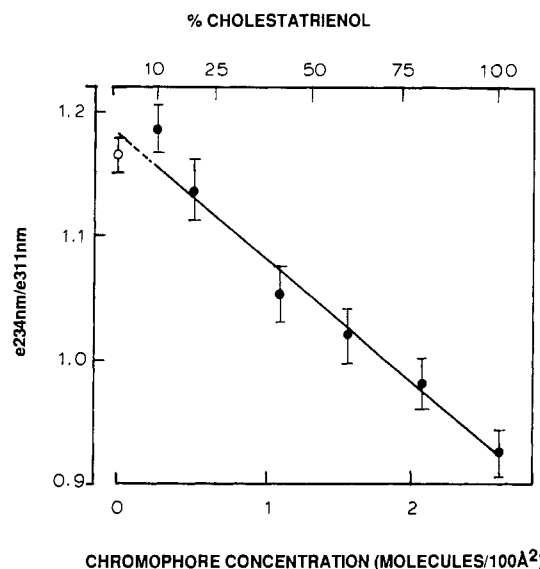

FIGURE 5: Absorption ratio of various cholestatrienol/cholesterol dispersions in buffer (●) and ethanol (○). Total sterol concentration was 5×10^{-5} M.

FIGURE 6: (Panel A) Absorption spectra of pyrenyl-PC in PC liposomes in buffer (−−) and ethanol (—). The absorption spectra demonstrate apparent hypochromicity and absorbance maxima red shift, due to light scattering by the liposome suspension. (Panel B) Absorption spectra of cholestatrienol/POPC (1:1) in buffer (−−). Absorption spectrum corrected for scattering artifacts (—) from data in panel A.

sorbance band pertinent to energy transfer was not significantly different from that of unassociated molecules in ethanol. The identical shapes of the resulting corrected and normalized emission spectra of cholestatrienol in ethanol and buffer indicate that the highly quenched (>90%) residual fluorescence emission from aqueous solutions of cholestatrienol (data not shown) arises from monomeric unassociated molecules and that the associated cholestatrienol aggregates formed in aqueous solution are dark complexes, as was concluded by Rogers et al. (1979).

The 324/311-nm absorbance ratio was calculated in various cholestatrienol/cholesterol mixtures (Figure 5) and was found to increase monotonically as the cholestatrienol became diluted. At 10 mol % cholestatrienol, the absorbance ratio was within experimental error of that of cholestatrienol in ethanol (open circles). These data are consistent with cholestatrienol freely mixing with the cholesterol aggregates.

(4) *Absorption Spectra of Cholestatrienol in POPC Liposomes.* Absorption spectra were obtained (Figure 6, dashed lines) for POPC/cholestatrienol (1:1) and for POPC containing 7.5 mol % pyrenyl-PC. The absorbance spectrum of pyrenyl-PC was then measured in ethanol at the same concentration (panel A, solid line). The cholestatrienol spectrum was then corrected for scattering artifacts (panel B, solid line),
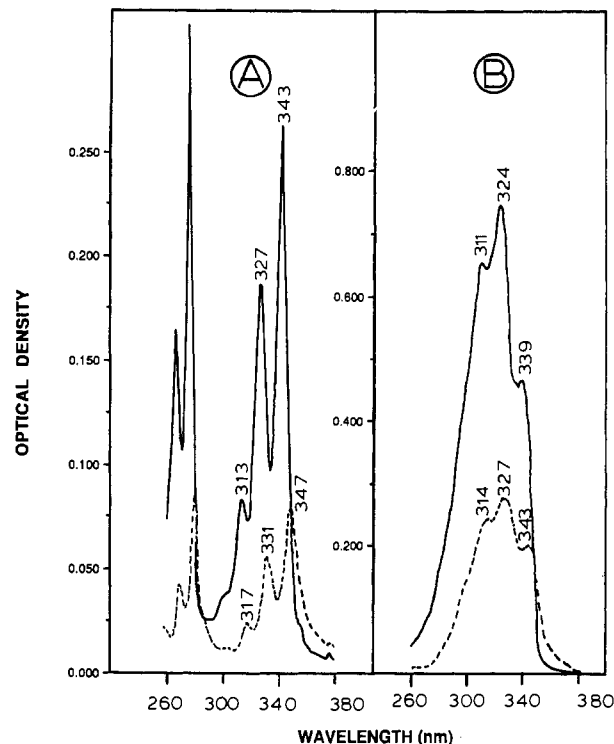
and both the 324/311-nm absorbance ratio and the molar extinction were found to be within experimental error of those obtained in ethanol (Figure 1).

At 1:1 POPC/cholestatrienol, the density of chromophores is approximately 1 molecule/100 Å². At a similar chromophore density in aqueous cholesterol aggregates, a marked reduction in the 324/311 absorbance ratio is observed (Figure 3, panel B). These data indicate that the cholestatrienol molecules in the POPC matrix, at a molar ratio up to 1:1, show no detectable electronic overlap of the triene π orbitals. If the cholestatrienol were dissolving in POPC to form a uniform mixture in a manner similar to its mixing with cholesterol, the absorbance ratio of cholestatrienol in POPC would be expected to be similar to that observed when cholestatrienol is mixed with cholesterol at the same concentration.

(5) *Time-Resolved Fluorescence Decay Measurements of Cholestatrienol in POPC Liposomes.* Time domain intensity decay curves were obtained for POPC sterol mixtures (1:1) containing cholestatrienol from 5 to 100% of the total sterol (2.5–50 mol % total lipid), at 12 concentrational increments at 37 °C. All fluorescence decay kinetics were fitted to single exponentials, and similar χ^2 values ($4.832 \times 10^{-2} \pm 0.624 \times 10^{-2}$) for the one-component data fit were obtained at all cholestatrienol concentrations.

The mean intensity rise time for the 12 experiments was 7.6 ± 3 ps. The fluorescence lifetimes at 37 °C were calculated from the curve fit, as described under Materials and Methods. A concentration-dependent decrease in lifetime was observed, such that at 2.5 and 520 mol % cholestatrienol the fluorescence lifetime had decreased from 644 to 560 ps, respectively.

Frequency domain lifetime studies of four separate liposome batches yielded lifetime decreases from 780 ± 25 to 700 ± 56 ps over the same concentration range of cholestatrienol. The background fluorescence (8–9-ns apparent lifetime) from
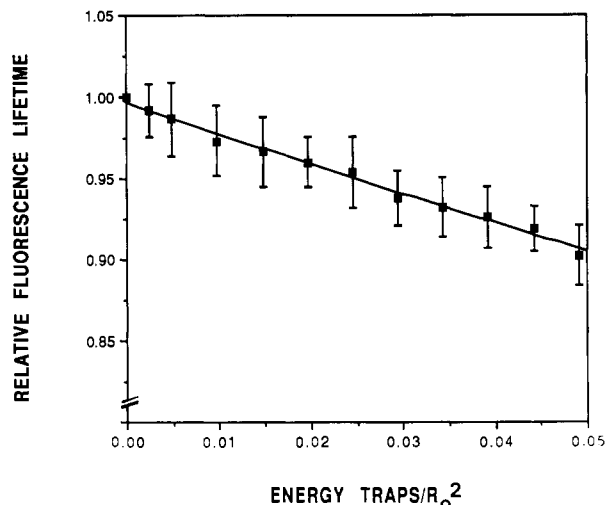
FIGURE 7: Phase and modulation lifetimes ($\pm$SD, $n = 5$) of varying concentrations of cholestatrienol in cholesterol/POPC liposomes at 37 °C. The total sterol/phospholipid ratio was 1:1. The abscissa is scaled to the number of bimolecular cholestatrienol energy traps expected to be present, calculated from eq 13.

FIGURE 8: ($\square$) Relative fluorescence intensities ($\pm$SD, $n = 5$) of varying concentrations of cholestatrienol in cholesterol/PC liposomes at 37 °C. The total sterol/phospholipid was 1:1. Also shown is the fitted exponential functions (no symbol) for the theoretical quantum yield, when these intensity measurements are corrected for loss of emitting fluorophores through bimolecular or tetramolecular energy traps estimated from the dynamic data (—).

lipids, buffer, and emission filters was resolvable by this technique, amounted to 1% of the cholestatrienol fractional intensity in the 2.5 mol % sample, and was present in samples without fluorescent probe. Two-component solutions to the experimental data yielded χ^2 values of <0.01. In all other samples (5–50 mol % cholestatrienol), the fractional intensity of the long-lifetime component was too weak to resolve, and two-component lifetime fits did not significantly improve χ^2. Phase and modulation lifetime results are shown in Figure 7. The abscissa is scaled to the apparent numbers of bimolecular traps present in the matrix expected to yield the observed quenching (lifetimes) curve, calculated from eq 13.

These independent techniques for measuring fluorescence lifetime are in good agreement. Time domain studies are particularly useful for analysis of rise times and contribution of relatively fast processes to the decay curves, while frequency domain measurements have advantages in the analysis of long-lived contributions to the intensity decay. These studies demonstrate that, within limits of detection, cholestatrienol emission in POPC/sterol liposomes is relatively homogeneous at all cholestatrienol/cholesterol ratios.

(6) Fluorescence Intensity Measurements of Cholestatrienol in POPC/Cholesterol Liposomes. Fractional steady-state emission intensity losses were significantly greater than the fractional decrease in fluorescence lifetime, particularly at the higher chromophore concentrations (>20 mol % cholestatrienol). At 50 mol % cholestatrienol, the emission intensity had decreased by 20%, whereas the fluorescence lifetime had decreased by only 10%. This result is consistent with energy loss through transfer to dark complexes of cholestatrienol, resulting in both reduction of fluorescence quantum yield and loss of total number of emitting fluorophores.

Fluorescence quantum yields should of course be identical whether measured by dynamic or by steady-state intensity measurements. Presented in Figure 8 is the experimental data from steady-state intensity measurements (open squares) and the resulting fit for the theoretical quantum yield, when these intensity measurements are corrected for loss of emitting fluorophores involved in bimolecular energy traps estimated directly from Figure 7.

For reasons discussed later (section 12 under Results), we also considered the situation for quaternary molecular traps, created for example by diffusion of a phospholipid molecule
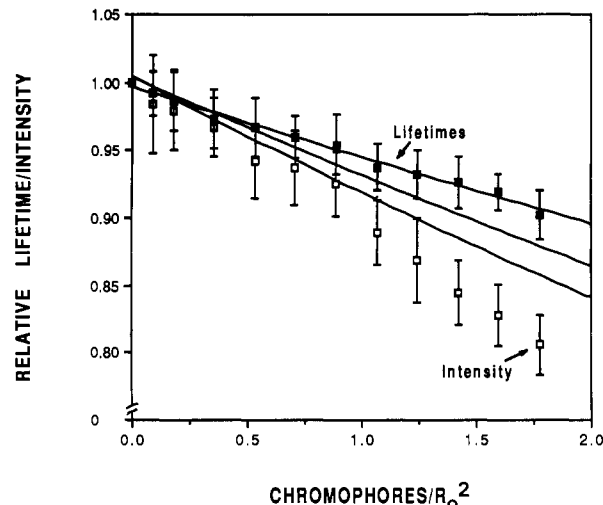
away from the center of a local sterol cluster. With the appropriate adjustment of R_0, rescaling the data in Figure 7, and adjustment of the total number of emitting fluorophores, the fit for the theoretical quantum yield corrected for losses created by tetramolecular energy traps is shown also in Figure 8. A significant improvement is obtained in interpreting the quenching data with these models, and indeed, the corrected intensity data utilizing a four-molecular trap can be considered statistically equivalent to the lifetime fit. Contributions from molecular collisions during the fluorescence lifetime contributing to dynamic quenching (estimated from the lipid diffusion coefficient given in section 2 under Theoretical and Experimental Considerations) are likely to be only marginal.

It must be kept in mind when a critical evaluation of the data is attempted (in terms of a particular quenching model) that the concentration of cholestatrienol of 50 mol % in POPC liposomes is equivalent to a (three dimensional) concentration of about 1.4 M. The observed quenching is thus relatively trivial when compared to the theoretical quenching expected from the density of energy traps created by direct molecular contacts in a random mixture of the two lipids (see next paragraph).

(7) Fluorescence Intensity Measurements of Cholestatrienol in Cholesterol Aggregates. The validity of assuming that quenching would occur to a greater degree in POPC liposomes if the molecules were free to adopt random proximity with each other is tested by utilizing cholesterol aggregates. Illustrated in Figure 9 (top panel) is the data obtained where the quenching profile of cholestatrienol in cholesterol aggregates (solid squares) is compared to that obtained with POPC (no symbol). In scaling the chromophore concentration with R_0^2 for the cholesterol aggregates, the value given to R_0 at each data point is corrected for quantum yield reduction (data not shown) from dynamic deactivation processes (determined by the decrease in fluorescence lifetime).

It is essential to realize the limitations of this comparison. Notwithstanding the uncertainty of the appropriate scaling of chromophore concentrations, other serious problems also exist. First, the fluorescence lifetime of cholestatrienol in cholesterol aggregates (1:200 mol/mol) is much longer (2.2 ns at 37 °C) than that in POPC, and this is likely to reflect different molecular environments of the probe (Nemecz &
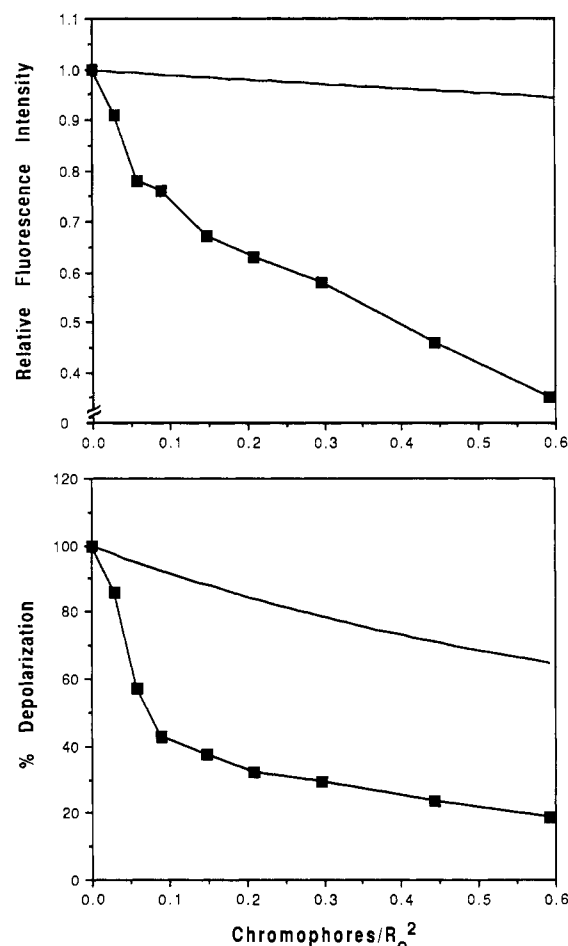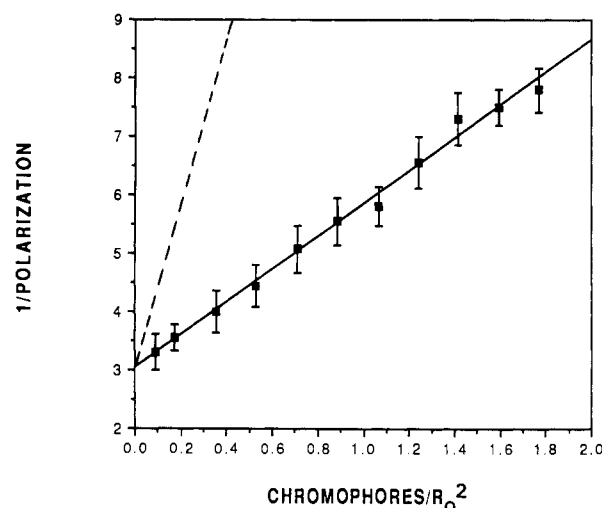
FIGURE 10: Concentration dependence of the depolarization of the fluorescence of cholestatrienol in POPC/cholesterol at 1:1 total sterol/phospholipid at 37 °C (±SD, n = 6). (—) Linear fit for data for calculation of slope and y intercept. (−−) Theoretical concentrational dependence of fluorescence depolarization calculated from eq 12 for no excluded volume between cholestatrienol molecular contacts (L = 7.05 Å).

FIGURE 9: (Top panel) Concentrational dependence of the relative fluorescence intensity (■) of cholestatrienol in cholesterol aggregates in buffer. (Bottom panel) Fluorescence depolarization measurements of cholestatrienol in cholesterol aggregates. Also shown on the plots are the respective intensities and depolarization of cholestatrienol in POPC/sterol liposomes (no symbol). The scaling of the abscissa is described in the text.

Schroeder, 1988). Second, the rotational motions are much slower in the aggregates than in POPC (section 11 under Results), and finally, the decrease in lifetime of cholestatrienol as a function of concentration in the aggregates was less than theoretically predicted from the degree of energy transfer and trap formation. (This may arise from photophysical artifacts generated by short-range electronic interactions between chromophores at the high concentrations encountered in the aggregates.)

Despite the assumptions that must be made in any direct comparison between these data sets, it is clear that random proximity of cholestatrienol molecules in POPC liposomes should result in much greater fluorescence quenching than is actually observed.

(*8*) *Dynamic Fluorescence Depolarization Measurements.* The multifrequency dynamic anisotropy data generated in this study clearly established that the decay of the emission anisotropy could only be modeled to a hindered rotator, since the fit to eq 2 was considerably better than that to eq 1 [in agreement with Schroeder et al. (1987) for dehydroergosterol in POPC], yielding r_∞ = 0.190 ± 0.003 (n = 4).

The apparent correlation time contributing to the anisotropy decay was 310 ± 120 ps and corresponds to rotational rates expected for the molecule embedded in POPC (introduction). Thus, the emission dipole is rapidly diffusing within a constrained environment of a cone angle of 23.1° (eq 3), yielding S = 0.77 (eq 4). This segmental order parameter agrees

closely with NMR data for the molecular order parameter of cholesterol (Taylor et al., 1982). These data indicate that the decay of fluorescence anisotropy is more sensitive to the hindered wobbling of the molecule around the short axis than the isotropic reorientations around the long axis. The *approximate* orientation of the transition dipoles therefore lie parallel in plane to the long molecular axis.

(*9*) *Fluorescence Depolarization Studies of Cholestatrienol in POPC/Sterol Liposomes.* The concentration-dependent depolarization of cholestatrienol fluorescence in 1:1 POPC/ sterol liposomes is shown in Figure 10. The data fit to an inverse function was highly correlated (r = 0.995). Theoretical polarization of cholestatrienol fluorescence in the absence of energy transfer (P_s), obtained from the intercept of the regression line, was 0.329 ± 0.022 polarization unit. The slope of the concentrational dependence of depolarization yielded a distance of closest approach of the probe molecules of 10.6 Å in sterol/POPC liposomes.

Also shown in the figure for reference is the concentrational dependence of the depolarization of fluorescence expected when cholestatrienol molecules are free to adopt their closest possible distance of approach (two molecular radii, or about 7 Å).

At a chromophore density of $0.0886/R_0^2$ (5 mol % cholestatrienol) in 1:1 POPC/sterol liposomes, energy transfer is sufficiently slow such that the polarization of fluorescence is within experimental error of the interpolated value of P_s. This information is helpful in choosing a reasonable concentration of cholestatrienol for dynamic depolarization measurements to determine molecular rotational rates.

(*10*) *Fluorescence Depolarization Studies of Cholestatrienol in POPC Liposomes.* Following evaluation of the transfer depolarization factor and R_0, each value of the fluorescence polarization of cholestatrienol at varying concentrations in POPC liposomes was corrected and scaled as described in section 5 under Theoretical and Experimental Considerations. The results of this analysis are shown in Figure 11. Shown on the figure is the best fit for the data points from the reciprocal plot in the upper panel, obtained for cholestatrienol in POPC/sterol liposomes at 1:1 molar ratio. It is clear from inspection of the overlap between the data obtained from the two studies that the slope of the depolarization curve in the
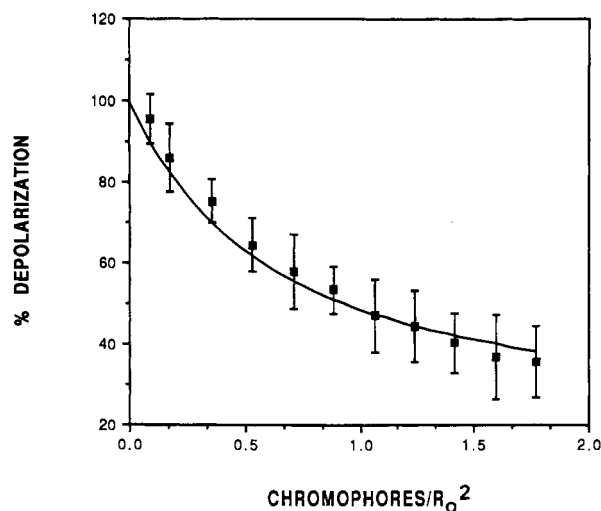
FIGURE 11: Depolarization of fluorescence of various cholestatrienol concentrations (2.5–50 mol %) in POPC liposomes ($\pm$SD, $n = 4$). Each data point (■) is corrected for orientational perturbations to energy-transfer efficiency induced by membrane ordering effects of increasing cholestatrienol concentration in the POPC lipid matrix. The reciprocal fit obtained in Figure 10 (no symbol) is shown on the plot for comparison.

absence of cholesterol is not any steeper at low chromophore densities. Thus, within the limits of detection, sterols do not appear to form clustered domains within the POPC phase at lipid/sterol ratios of less than 1:1.

(*11*) *Fluorescence Depolarization Studies of Cholestatrienol in Cholesterol Aggregates*. The steady-state anisotropy of cholestatrienol in cholesterol aggregates at 37 °C at 1:200 mol/mol of cholesterol is 0.323. Thus, the average displacement of the emission dipole (Lakowicz, 1983) is about 16° during the excited-state lifetime (2.2 ns). These molecular motions were too slow to accurately analyze in more detail by dynamic methods available.

In Figure 9 (bottom panel) a direct comparison of the concentrational dependence of the depolarization data in cholesterol aggregates (solid squares) with the fit to the concentrational dependence in POPC liposomes (no symbol) is presented. Clearly, given the experimental limitations, the rates of energy transfer appear to be much greater in the aggregates than in POPC at any given chromophore concentration.

The observation that both significant quenching and energy transfer occur at relatively low chromophore concentrations indicates that it is reasonable to utilize an intermediate value of the orientation factor for the calculation of R_0 for cholestatrienol in cholesterol aggregates. On the one hand, the orientation of the molecules must be sufficiently favorable such that quenched dark complexes form ($K \gg 0$) and, on the other, the orientation cannot be highly favorable since energy transfer between chromophores is strongly depolarizing ($K \ll 2$).

(*12*) *Model of Cholesterol Phospholipid Organization*. A regular crystalline lattice (upper panel) and a random liquid mixture (lower panel) of POPC/cholesterol (1:1) are depicted in Figure 12. The relative molecular diameters utilized in constructing these models are estimated from surface pressure measurements. As rotations of the sterol molecule around its long axis are faster than its wobbling motions (introduction), then on the nanosecond time scale the cross-sectional areas of these molecules can be considered uniform, with respect to the wobble of the sterol. The phospholipid molecular rotations are somewhat slower than the wobbling motions of cholesterol. However, due to the inherent flexibility of the acyl chain segments, a uniform representation of the diameters on the
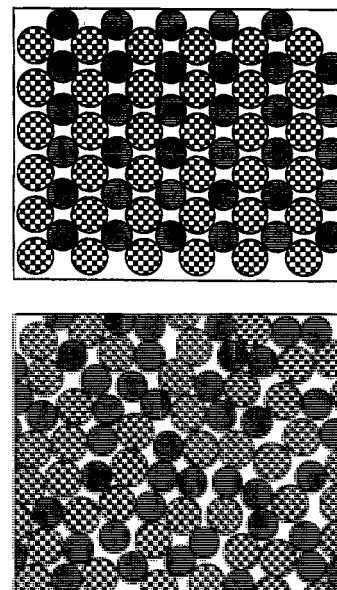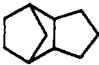

FIGURE 12: Models of extremes of molecular organization of cholesterol in POPC lipid bilayers. (Top panel) Crystalline lattice of equimolar mixtures of cholesterol/cholestatrienol (hatched circles) and POPC (checkered circles), at 37 °C. (Bottom panel) Random mixture of the two constituent lipids. The relative molecular diameters (Results, section 2) were estimated from surface pressure measurements of monolayers of the mixture and sterols alone.

nanosecond time scale applies when the phospholipid acyl chain electronic distribution is viewed as an average over all segments.

The crystalline lattice constructed from the above data will have sterol molecules separated by distances of 9.7 and 12.3 Å (rows) and 15.8 Å (diagonals), whereas in a random mixture there are molecular contacts between most of the cholesterol molecules. At 1:1 sterol/phospholipid, due to the limited geometrical arrangements possible, we conclude that cholesterol is organized in the phospholipid phase in a manner similar to that depicted for a regular crystalline lattice. The mesomorphic rather than crystalline state of the lipid matrix would be likely to result in a less defined identity between rows of lipid, such that the average distance between rows of the sterol molecules would be about $(9.7 + 12.3)/2 = 11$ Å. Thus, the experimentally determined distance of 10.6 Å is reasonably consistent with such a model. (Note: The diffusion of one phospholipid molecule away from its putative lattice site will result in a tetramolecular energy trap, referred to in section 6 under Results.)

(*13*) *Estimation of the Relative Attractive Forces between Acyl Chains and Cholesterol*. Examination of Hoy's revision of Small's tables (Hoy, 1970; Small, 1953) indicates that many of the hydrophobic group features of the sterol molecule, as well as the structure features, have *less* molar attraction than features between the methylene segments of the acyl chains (Table II). For example, the average molar attraction of each unit of the sterol and acyl chain is approximately 114 and 158 $(cal/cm^3)^{1/2}/mol$, respectively. It is also likely that the structural features of the cholesterol molecule (note the general similarity to the structure feature given in Table II) may have a strong influence on the Hildebrand solubility parameter. Thus, the location of a sterol molecule within the vicinity of a phospholipid molecule is likely to promote both stronger inter- and stronger intramolecular associations of methylene segments within the same or neighboring phospholipid molecules, contributing to the reduction in both the mean molecular area and reduced radius of gyration of the acyl chains by the presence of cholesterol.

Table II: Group Molar Attraction Constants of Various Structural Groups in Fatty Acyl Chains and Sterol Molecules[a]

group or structure feature	molar attraction $[(cal/cm^3)^{1/2}/mol]$
$-CH_3$	147.3
$-CH_2-$	131.5
$>CH-$	85.99
$>C<$	32.03
$-CH=$	121.53
$-COO-$	326.58
$-OH$	225.84
	62.5

[a] The data in the table are taken directly from Hoy (1970).

DISCUSSION

In this study, we utilize the concentrational dependence of fluorescence depolarization to monitor excitation transport between chromophores. From comparison of experimental data to a mathematical model whereby the chromophores are constrained by a minimum separation distance, we conclude that sterol molecules are separated by an average distance of 10.6 Å in the bilayer at 1:1 sterol/POPC. The methods used in this study to estimate the intersterol molecular distances rely on the validity of the applicability of the Forster theory of singlet transfer of radiation between cholestatrienol molecules. While we have attempted to demonstrate that Forster's theory can indeed account for energy transfer rates between randomly distributed chromophores in cholesterol aggregates, the validity of the comparison must await further analysis of the precise molecular arrangements and motion of molecules in these aggregates. Our concern for unequivocally demonstrating the applicability of Forster's theory arises from R_0 being somewhat smaller than is customarily experienced in calculations of this nature. However, Eisinger et al. (1969) concluded that for aromatic amino acid hetero- and homomolecular energy transfer ($5 Å < R_0 < 25 Å$), for $R_0 > 10$ Å, the transfer rate can be accounted for by the Forster mechanism, as long as the separation distance exceeds about 5 Å.

Other investigators have also monitored the steady-state depolarization of fluorescent sterols at various concentrations in the absence of cholesterol (Rogers et al., 1979; Schroeder et al., 1987; Smutzer, 1988). In the study by Rogers et al. (1979), the authors determined that the magnitude of the observed fluorescence depolarization indicated that the sterol molecules were ordered in DPPC in such a way that overlap of the π orbitals between adjacent sterol molecules was inhibited. The model of sterol organization proposed by these authors was that the cholesterol molecules formed connected rows within the phospholipid matrix. The rapid rotations of sterol molecules detected by NMR (Taylor et al., 1981, Duforc et al., 1984) and dynamic depolarization studies (Schroeder et al., 1987; this study) occurring at times around the fluorescence lifetime indicate that the anomalous slow rate of energy transfer observed at relatively high fluorescent sterol concentration is unlikely to arise from an unfavorable relative molecular orientation. However, the data presented here confirm the general interpretation of these authors, and it has been our intent to build upon this key study with an attempt at a more quantitative approach to the analysis. Schroeder et al. (1987) concluded from similar experiments presented by Rogers et al. (1979) that sterol molecules could not be aggregated in POPC SUV's, and the data presented here confirm these findings.

The organization of sterol molecules in the membrane matrix has also been discussed by Presti et al. (1982a,b), at a 1:1 sterol/phospholipid molar ratio. The organization presented by the authors was postulated to arise from 1:1 complex formation with the phospholipid. This interpretation is supported by a variety of biophysical studies [see the introduction and Presti et al. (1982a,b)], in as much as the full participation of both phospholipid and cholesterol in the interaction is required to account for the thermodynamic behavior of the systems under study. Such a static view of the interaction between sterols and phospholipids has been criticized (Yeagle, 1981) on the grounds that the rotational correlation times of the two species are sufficiently different to make such an interaction (i.e., a 1:1 complex) untenable.

In this study, we suggest from our data and also from geometrical considerations that sterol molecules are disconnected and average four phospholipid acyl chains as nearest neighbors, while each acyl chain forms pair contacts with an average of four cholesterol molecules and four acyl chains from the same or neighboring phospholipid molecules. We term this arrangement an "ordered bimolecular mesomorphic lattice" and it may be a special case among the more general smectic type B liquid crystalline mesophases thus far described.

At sterol concentrations less than 1:1, we find no evidence for formation of sterol-rich domains in the lipid matrix (we do not mean to imply that regions of cholesterol inhomogeneity do not exist in other systems, e.g., biological membranes, where the influence of the many polydispersed components on cholesterol phase behavior is obviously much more complicated). Also, the ordering effects of cholesterol are apparently equally effective over a wide range of sterol concentrations (Figure 2). Thus, we conclude that local interactions between cholesterol and acyl chains appear to mediate the condensing/ordering effects of cholesterol.

These interactions are likely to be dominated by the dispersion forces (London–van der Waals') between the sterol and acyl chains (introduction). If, for example, the sterol/acyl chain interaction strength is greater than that between acyl chain segments, steric effects might promote correlated motions between the two molecules, as suggested by Dufourc et al. (1984). Alternatively, acyl chain condensation could result from the interaction strength between the methylene segments of the acyl chains being greater than those between sterol molecules and methylene units. Condensation of the acyl chains in this case might arise from increased mutual interpenatratability of the methylene segments resulting from the juxtaposed cholesterol molecules being less attractive to the acyl chain segments than the original displaced phospholipid molecules. Indeed, the resulting Hildebrand solubility parameters (i.e., the group molar attraction constants summed over all interacting molecular segments) obtained from Table II indicate that this is indeed the more likely explanation.

As molecular dispersion forces are additive, the "poor solvent" effect of cholesterol molecules located on an ordered mesomorphic lattice would be expected to be distributed among several nearest-neighbor acyl chains, while each acyl chain would experience the additive effect of more than one sterol molecule. The apparent homogeneous distribution of cholesterol on lattice sites in the bulk lipid matrix at sterol/phospholipid ratios less than 1:1 and the lack of sterol/sterol pair contacts would therefore result in the maximum distribution and effectiveness of the dispersion forces over a wide range of cholesterol concentrations. Thus, the lattice arrangement may be a prerequisite for efficient molecular interactions of cholesterol producing the condensing effects at increasingly higher mole fraction of sterol. Also, the condensing effects of sterols would be expected to be greatest when the surface

area contact between the cholesterol molecules and acyl chains is maximized. At increasingly high sterol concentrations, this would occur when sterol molecules are arranged in the proposed configuration. These factors may provide an explanation for the proportionality of the ordering effects of cholesterol up to approximately 1:1 mol/mol of phospholipid, where all available sterol sites for this particular molecular arrangement become filled.

These considerations indicate that evaluation of the chemical thermodynamic properties of the lipid components would assist prediction of the behavior of cholesterol in phospholipid bilayers. For example (with reference to a hypothetical random noncondensed mixture of the two lipids), it seems likely that the enthalpy decrease associated with reduction in the motional degrees of freedom of the acyl chains in the presence of cholesterol and the negative entropy associated with loss of both acyl chain molecular volume and ordered lattice formation are interdependent. The particular molecular organization of the lipid matrix that might arise from counterbalancing the energetic and statistical parameters could be influenced by a driving force toward a configuration of lower energy. The isolated sterol molecule surrounded by four phospholipid molecules may represent an appropriate molecular arrangement at a potential energy minima for two possible reasons: First, from simple rigid cylinder geometrical considerations the proposed ordered mesomorphic lattice arrangement minimizes the free volume between molecules (and therefore the cohesive contact between molecules is maximized). Second, sterol/acyl chain cohesive forces would (from the gmac arguments) be stronger than those between sterol molecules, contributing to the stability of cholesterol molecules in a potential energy well.

The relative differences in the magnitude of segmental intermolecular cohesive forces capable of producing relative molecular attractions and repulsions that give rise to different degrees of interpenatratability of the flexible acyl chain segments need only be subtle. Structural modification to the components, therefore, is likely to produce observable changes to the magnitude of the effects of sterols. Thus, addition of chemical groups to the sterol or acyl chains that alters the molar attraction of the molecular segments or modifies the relative flexibility of the acyl chain segments would both be expected to influence the behavior of acyl chain interpenetration in the presence of cholesterol molecules. An example of modified phospholipids exhibiting this behavior would perhaps be represented by docosahexaenoyl-PC, which is not condensed by cholesterol (Demel et al., 1972). The molar attraction constant of the six —C=C— segments are lower than those of their methylenic counterparts (Table II), and for steric reasons, the flexibility of the segments of this lipid are much reduced compared to other naturally occurring acyl chains (Applegate & Glomset, 1986; Hyslop, 1981).

In conclusion, the unique structural features of the mesomorphic molecular ensemble of the phospholipid/cholesterol bilayer, combining the effects of condensed acyl chains and a regular array of rigid cholesterol molecules, result in a highly ordered lipid matrix. The condensing effect of the juxtaposed cholesterol molecules is postulated to arise from increased interpenetration of the acyl chain segments between neighboring phospholipid molecules. We suggest that the interdependence of the condensing effects and formation of the ordered mesomorphic lattice may represent some of the necessary conditions governing the effects of sterols on the physical and mechanical properties of condensable phospholipids and biological membranes in the fluid phase.

REFERENCES

Aloia, R. C., Jensen, F. C., Curtain, C. C., Mobley, P. W., & Gordon, L. M. (1988) *Proc. Natl. Acad. Sci. U.S.A. 85*, 900–904.

Applegate, K. R., & Glomset, J. A. (1986) *J. Lipid Res. 27*, 658–680.

Antonucci, R., Bernstein, S., Giancola, D., & Sax, K. J. (1951) *J. Org. Chem. 16*, 1159–1164.

Backer, J. M., & Dawidowicz, E. A. (1979) *Biochim. Biophys. Acta 551*, 260–270.

Birks, J. B., & Dyson, D. J. (1963) *Proc. R. Soc. London, A 275*, 135–148.

Bittman, R., Clejan, S., Lund-Katz, S., & Phillips, M. C. (1984) *Biochim. Biophys. Acta 772*, 117–126.

Bourges, M., Small, D. M., & Dervichian, D. G. (1967) *Biochim. Biophys. Acta 137*, 157–161.

Bowen, E. J. (1950) *Q. Rev., Chem. Soc. 4*, 236–243.

Connolly, T. J., Carruthers, A., & Melchior, D. L. (1985) *Biochemistry 24*, 2865–2873.

Crews, F. T., McElhaney, M. R., Klepner, C. A., & Lippa, A. S. (1988) *Drug Dev. Res. 14*, 31–44.

Dale, R. E., & Eisenger, J. (1975) in *Biochemical Fluorescence: Concepts* (Chen, R. F., & Edelhoch, H., Eds.) Vol. 1, Chapter 4, pp 115–284, Marcel Dekker, New York.

Darke, A., Finer, E. G., Flook, A. G., & Phillips, M. C. (1972) *J. Mol. Biol. 63*, 265–280.

Davis, J. H. (1983) *Biochim. Biophys. Acta 737*, 117–171.

De Gier, J., Mandersloot, J. G., & van Deenen, L. L. M. (1968) *Biochim. Biophys. Acta 150*, 666–675.

Demel, R. A., & De Kruyff, B. (1976) *Biochim. Biophys. Acta 457*, 109–132.

Demel, R. A., Geurts Van Kessel, W. S. M., & Van Deenen, L. L. M. (1972) *Biochim. Biophys. Acta 266*, 26–40.

Dufourc, E. J., Parish, E. J., Chitrakorn, S., & Smith, I. C. P. (1984) *Biochemistry 23*, 6062–6071.

Eisinger, J., Feuer, B., & Lamola, A. A. (1969) *Biochemistry 10*, 3908–3915.

El-Sayed, M. Y., Guion, T. A., & Fayer, M. D. (1986) *Biochemistry 25*, 4825–4832.

Farias, R. N., Bloj, B., Sineriz, F., & Trucco, R. (1975) *Biochim. Biophys. Acta 415*, 231–241.

Flory, P. J. (1942) *J. Chem. Phys. 10*, 51–58.

Flory, P. J. (1983) *Principals of Polymer Chemistry*, Chapters 10–12, Cornell University Press, Ithaca, NY.

Flory, P. J., & Krigbaum, W. R. (1950) *J. Chem. Phys. 18*, 1086–1096.

Forster, T. (1948) *Ann. Phys. (Leipzig) 2*, 55–75.

Gordon, L. M., & Sauerheber, R. D. (1977) *Biochim. Biophys. Acta 466*, 34–43.

Gratton, E., Lakowicz, J. R., Maliwal, B., Cherek, H., Laczko, G., & Limkeman, M. (1984) *Biophys. J. 446*, 479–486.

Hale, J. E., & Schroeder, F. (1982) *Eur. J. Biochem. 122*, 649–661.

Hildebrand, J. H., & Scott, R. L. (1962) *Regular Solutions*, Prentice-Hall, Englewood Cliffs, NJ.

Hresko, R. C., Sugar, I. P., Barenholz, Y., & Thompson, T. E. (1986) *Biochemistry 25*, 3813–3823.

Hoy, K. L. (1970) *J. Paint Technol. 42*, 76–118.

Hubble, W. L., & McConnell, H. M. (1971) *J. Am. Chem. Soc. 93*, 314–326.

Hui, S. W., & Parsons, D. F. (1975) *Science 190*, 383–384.

Hyslop, P. A. (1981) Ph.D. Thesis, University of Southampton, Southampton, U.K.

Jacobs, R., & Oldfield, E. (1979) *Biochemistry 18*, 3280–3285.

Jain, M. K. (1988) *Introduction to Biological Membranes*, Chapter 5, Wiley-Interscience, New York.

Jain, M. K., & White, H. B. (1977) *Adv. Lipid Res. 15*, 1–60.

Krause, S. (1978) in *Polymer Blends*, Vol. 1, Polymer-Polymer compatability (Paul, D. R., ed) Academic Press, New York.

Ladbrooke, B. D., Williams, R. M., & Chapman, D. (1968) *Biochim. Biophys. Acta 150*, 333–340.

Lakowicz, J. R. (1983) in *Principals of Fluorescence Spectroscopy*, Plenum Press, New York.

Lakowicz, J. R., & Prendergast, F. G. (1978) *Science 200*, 1399–1401.

Lakowicz, J. R., Prendergast, F. G., & Hogan, D. (1979) *Biochemistry 18*, 520–527.

Lakowicz, J. R., Cherek, H., & Balter, A. (1981) *J. Biochem. Biophys. Methods 5*, 131–146.

Larsen, E. S., & Berman, H. (1934) *U.S. Geol. Surv. Bull. 848*, 11–54.

Lecuyer, H., & Dervichian, D. G. (1969) *J. Mol. Biol. 45*, 39–57.

Mabrey, S., Mateo, P. L., & Sturtevant, J. M. (1978) *Biochemistry 17*, 2464–2468.

Marcelja, S. (1974) *Biochim. Biophys. Acta 367*, 165–176.

McLeod, A. J., Suckling, K. E., Walton, P. L., & Johnson, M. (1982) *Biochim. Biophys. Acta 688*, 581–585.

Muller-Landau, F., & Cadenhead, D. A. (1979) *Chem. Phys. Lipids 25*, 315–328.

Nemecz, G., & Schroeder, F. (1988) *Biochemistry 27*, 7740–7749.

Pal, R., Barenholz, Y., & Wagner, R. R. (1981) *Biochemistry 20*, 520–539.

Pink, D. A., Green, T. J., & Chapman, D. (1981) *Biochemistry 20*, 6692–6698.

Poznansky, M., & Lange, Y. (1976) *Nature 259*, 420–421.

Presti, F. T., Pace, R. J., & Chan, S. I. (1982a) *Biochemistry 21*, 3821–3830.

Presti, F. T., Pace, R. J., & Chan, S. I. (1982b) *Biochemistry 21*, 3831–3835.

Renshaw, P. F., Janoff, A. S., & Miller, K. W. (1983) *J. Lipid Res. 24*, 47–51.

Rogers, J., Lee, A. G., & Wilton, D. (1979) *Biochim. Biophys. Acta 552*, 23–37.

Rottem, S., Cirillo, V. P., & de Kruyff, B. (1973) *Biochim. Biophys. Acta 323*, 509–519.

Sauerheber, R. D., Gordon, L. M., Crosland, R. D., & Kuwahara, M. D. (1977) *J. Membr. Biol. 31*, 131–169.

Schroeder, F. (1984) *Prog. Lipid Res. 23*, 97–113.

Schroeder, F., Dempsey, M. E., & Fischer, R. T. (1985) *J. Biol. Chem. 260*, 2904–2911.

Schroeder, F., Barenholz, Y., Gratton, E., & Thompson, T. E. (1987) *Biochemistry 26*, 2442–2448.

Small, P. A. (1953) *J. Appl. Chem. 3*, 75–95.

Smutzer, G. (1988) *Biochim. Biophys. Acta 946*, 270–288.

Snyder, B., & Freire, E. (1982) *Biophys. J. 40*, 137–148.

Stockton, G. W., & Smith, I. C. P. (1976) *Chem. Phys. Lipids 17*, 251–263.

Strickler, S. J., & Berg, R. A. (1962) *J. Chem. Phys. 37*, 814–822.

Su, S.-G., & Simon, J. D. (1987) *J. Phys. Chem. 91*, 2693–2696.

Tanford, C. (1961) in *Physical Chemistry of Macromolecules*, Chapter 4, Wiley, New York.

Taylor, M. G., Akiyama, T., & Smith, I. C. P. (1981) *Chem. Phys. Lipids 29*, 327–339.

Taylor, M. G., Akiyama, T., Saito, H., & Smith, I. C. P. (1982) *Chem. Phys. Lipids 31*, 359–379.

Weber, G. (1954) *Trans. Faraday Soc. 50*, 552–555.

Weber, G. (1978) *Acta Phys. Pol., A 54*, 173–178.

Whetton, A. D., & Houslay, M. D. (1983) *FEBS Lett. 157*, 70–74.

Worcester, D. L., & Franks, N. P. (1976) *J. Mol. Biol. 100*, 359–378.

Yeagle, P. L. (1981) *Biochim. Biophys. Acta 640*, 263–273.

Yeagle, P. L. (1985) *Biochim. Biophys. Acta 822*, 267–287.

Yin, J.-J., Feix, J. B., & Hyde, J. S. (1987) *Biophys. J. 52*, 1031–1038.